Chinese Journal of Cancer Research
2022 Impact Factor: 5.1
Journal Citation Reports™, Clarivate Analytics

Striatins and STRIPAK complex partners in clinical outcomes of patients with breast cancer and responses to drug treatment

Amber Xinyu Li, Jimmy Jianyuan Zeng, Tracey A Martin, Lin Ye, Fiona Ruge, Andrew J Sanders, Elyas Khan, Q. Ping Dou, Eleri Davies, Wen G Jiang

Citation: Amber Xinyu Li, Jimmy Jianyuan Zeng, Tracey A Martin, Lin Ye, Fiona Ruge, Andrew J Sanders, Elyas Khan, Q. Ping Dou, Eleri Davies, Wen G Jiang. Striatins and STRIPAK complex partners in clinical outcomes of patients with breast cancer and responses to drug treatment. *Chin J Cancer Res* 2023; 35(4): 365–385. doi: 10.21147/j.issn.1000–9604.2023.04.04

View online: http://article.cjcrcn.org/article/doi/10.21147/j.issn.1000–9604.2023.04.04

Original Article

Striatins and STRIPAK complex partners in clinical outcomes of patients with breast cancer and responses to drug treatment

Amber Xinyu Li[1], Jimmy Jianyuan Zeng[1], Tracey A Martin[1], Lin Ye[1], Fiona Ruge[1], Andrew J Sanders[1,2], Elyas Khan[3], Q. Ping Dou[1,3], Eleri Davies[4], Wen G Jiang[1]

[1]Cardiff China Medical Research Collaborative, Division of Cancer and Genetics, Cardiff University School of Medicine, Heath Park, Cardiff CF14 4XN, UK; [2]School of Natural and Social Science, University of Gloucestershire, Francis Close Hall, Cheltenham GL50 4AZ, UK; [3]Karmanos Cancer Institute, Department of Oncology, School of Medicine, Wayne State University, Detroit MI 48201, USA; [4]Wales Breast Center, Cardiff and Vales University Health Board, University Llandough Hospital, Cardiff CF64 2XX, UK

Correspondence to: Prof. Wen G Jiang. Cardiff China Medical Research Collaborative, Division of Cancer and Genetics, Cardiff University School of Medicine, Heath Park, Cardiff CF14 4XN, UK. Email: jiangw@cardiff.ac.uk.

Abstract

Objective: Striatins (STRNs) family, which contains three multi-domain scaffolding proteins, are cornerstones of the striatins interacting phosphatase and kinase (STRIPAK) complex. Although the role of the STRIPAK complex in cancer has become recognized in recent years, its clinical significance in breast cancer has not been fully established.

Methods: Using a freshly frozen breast cancer tissue cohort containing both cancerous and adjacent normal mammary tissues, we quantitatively evaluated the transcript-level expression of all members within the STRIPAK complex along with some key interacting and regulatory proteins of STRNs. The expression profile of each molecule and the integrated pattern of the complex members were assessed against the clinical-pathological factors of the patients. The Cancer Genome Atlas (TCGA) dataset was used to evaluate the breast cancer patients' response to chemotherapies. Four human breast cancer cell lines, MDA-MB-231, MDA-MB-361, MCF-7, and SK-BR-3, were subsequently adopted for *in vitro* work.

Results: Here we found that high-level expressions of STRIP2, calmodulin, CCM3, MINK1 and SLMAP were respectively associated with shorter overall survival (OS) of patients. Although the similar pattern observed for STRN3, STRN4 and a contrary pattern observed for PPP2CA, PPP2CB and PPPR1A were not significant, the integrated expression profile of STRNs group and PPP2 group members constitutes a highly significant prognostic indicator for OS [P<0.001, hazard ratio (HR)=2.04, 95% confidence interval (95% CI), 1.36−3.07] and disease-free survival (DFS) (P=0.003, HR=1.40, 95% CI, 1.12−1.75). Reduced expression of STRN3 has an influence on the biological functions including adhesiveness and migration. In line with our clinical findings, the breast cancer cells responded to STRN3 knockdown with changes in their chemo-sensitivity, of which the response is also breast cancer subtype dependent.

Conclusions: Our results suggest a possible role of the STRIPAK complex in breast cancer development and prognosis. Among the members, the expression profile of STRN3 presents a valuable factor for assessing patients' responses to drug treatment.

Keywords: Striatins; STRN3; STRIPAK; breast cancer; prognosis; chemo-resistance

Submitted Jul 14, 2023. Accepted for publication Aug 15, 2023.
doi: 10.21147/j.issn.1000-9604.2023.04.04
View this article at: https://doi.org/10.21147/j.issn.1000-9604.2023.04.04

Introduction

The investigation on the striatins (STRNs) family arose from two decades ago when Muro *et al.* identified a protein, which is now known as striatin-3 (STRN3 or SG2NA), during the S and G2 phase of the cell cycle by using antibodies acquired from cancer patient (1). While this study was being conducted, another research, which speculated the activities of adenylyl cyclase at the synapses, had coincidently discovered a WD-repeat family protein, called STRN, highly expressed at the dendritic sites in rat brain (2). The final member constituting the STRNs family, zinedin, was discovered in 2000 and was renamed later as striatin-4 (STRN4) (3). The three STRNs are homologous proteins that contain similar number of amino acids and possess identical interacting domain structure including a caveolin-binding domain, a coiled-coil region, a calmodulin (CaM, or CALM1) binding domain and a WD-repeat domain. Consistent with the presence of those domains, STRNs appear to associate with caveolin-1 and calmodulin in a Ca^{2+} dependent manner (4,5). It is now established that the members within the STRNs family are both cytosolic and membrane-bound proteins, and recently STRNs have also been suggested to function as cell adhesion regulators at both adherens junctions and tight junctions in epithelial cells (3,6). Although the full functions of STRNs were not entirely clear, the findings that they interacted with protein phosphatases, namely protein phosphatase 2A (PP2A) (coded by the *PPP2CA* gene) and PP2B (protein phosphatase 2B) (coded by the *PPP2CB* gene) indicated their role in regulating the phosphatases and phosphorylation events.

In terms of signalling partners, perhaps the most important discovery is that STRNs, particularly STRN3 is a cornerstone protein for the STRIPAK complex (the striatin-interacting phosphatases and kinases). The STRIPAK complex contains a rather large number of subunit proteins sufficiently linked by STRN3 via their coiled duplex domain, which is a region serves as platform allowing other partners to dock (7,8). Some of the well-known STRIPAK members are STRN3, calmodulin, PP2A, caveolin, MOB4 and GCKIII. While in recent years, cerebral cavernous malformations 3 [CCM3, or programmed cell death protein 10 (PDCD10)], sarcoma associated protein (SLMAP), striatin interacting proteins 1 [STRIP1, or family with sequence similarity 40 member A (FAM40A)], striatin interacting proteins 2 (STRIP2 or FAM40B), PP2CB, PP2A regulatory subunit A (PPP2R1A), cortactin binding protein 2 (CTTNBP2), macrophage stimulating-1 [MST1 or hepatocyte growth factor like protein (HGFL)], suppressor of IKK epsilon (SIKE1) and misshapen like kinase 1 (MINK1) were also reported to be closely or loosely associated with the STRIPAK complex and are also regarded as the STRIPAK partners (9-11). The functions of STRNs and STRIPAK are not entirely clear but with the number and complex pattern of the interacting partners, their function is likely complex and diverse.

STRNs are known to bind with caveolin and calmodulin, contributing to T-cell proliferation and Ca^{2+} dependent tissue activation (5). Gordon *et al*. have claimed that STRN is able to orchestrate the regulation of CCM3 and MST3 by PP2A (12). SLMAP, as part of the STRIPAK complex, has also been implicated in cell-cycle control (13). A recent study conducted by Lahav-Ariel *et al.* showed that STRN may be poly-ADP-ribosylated following interaction with Tankyrase 1 (TNKS1) (6). STRN and MOB4 (Mps one binder kinase activator family member 4) together could coordinate the Wnt signalling pathway and play a role in embryonic development (14). STRIPAK is also involved in the Hippo signalling event and the Hippo-STRIPAK complex could act on DNA double-stranded break repair and genomic stability (15,16).

In colon epithelial cells, STRN was found to colocalize with adenomatous polyposis coli (APC), while targeting either STRN or APC impeded the tight junctional functions in these cells (17). Additionally, knocking down STRN inhibited cell migration of endothelial cells (18). This regulation of adhesion by STRN seems to involve both tight junctions and adherens junctions and possibly the interactive relationship between the two important cell adhesion and permeability structures (6). Moreover, the anchoring of the membrane localized ER mediated by its interaction with STRN has been suggested to facilitate breast cancer cell survival, proliferation and endocrine resistance (19).

The role of the STRIPAK complex in cancer is becoming recognized in recent years. In clinical cancer and database analyses, STRIPAK was thought to be a possible oncogenic complex in liver hepatocellular carcinoma (HCC) and renal clear cell carcinoma (RCCC) (20). STRN4 was found to aberrantly affect liver HCC cells and STRN4 suppression resulted in reduction of tumorigenicity of these liver cancer cells (21). Ito *et al*. have recently reported the appearance of an anti-STRN4 antibody in patients with esophageal cancer and the

antibody levels appear to have both diagnostic and prognostic values for esophageal squamous cell carcinoma (ESCC) (22). In thyroid cancer, it has been shown that the complex gene rearrangement resulted in the formation of a STRN-ALK kinase fusion protein, allowing ALK activation and promoting tumor formation (23). Qiu *et al*. have shown that STRIP2 is also an oncogenic player for lung adenocarcinoma cells (24).

There are several pathways that STRNs participate in the regulation of cellular functions in cancer cells. In pancreatic cancer cells, STRN4 knockdown suppressed cell growth and invasion (25). Of a particular interest is the connection between STRNs and cancer cells response to drug treatment. Knocking down STRN4 in pancreatic cancer cells increased the sensitivity of cells to gemcitabine (25). In breast cancer cell line, MCF-7, targeting the functional form of STRN3 protein by truncated protein, confers EMT transformation of the cells (26).

The link between STRNs and drug response in breast cancer has not been fully explored. Breast cancer tissues have been shown to possibly express different variant forms of the STRN3 proteins, which in turn may involve in diverse signalling events (27). There is a good reason that STRNs and STRIPAK members may play a role in breast cancer. STRNs family members have been shown to serve as scaffolds for formation of protein complexes between PP2A and estrogen receptor (ER), ERα (28,29). Estrogen, via ERα, is a central player in the development and progression of breast cancer, a connection established for almost a century. Beyond this connection, the multiple biological functions played by STRNs and STRIPAK partners also suggest that the STRIPAK complex may play an important role in breast cancer.

Most of the previous studies have examined individual members of the STRIPAK family. There have been no reports on the comprehensive analysis of the STRPAK complex members in any cancer type. Therefore, the present study collectively explored the expression of a cohort of STRIPAK complex members in breast cancer and examined the clinical and potential therapeutic values of these molecules.

Materials and methods

Cell lines

Four human breast cancer cell lines, namely MDA-MB-231, MDA-MB-361, MCF-7 and SK-BR-3 were obtained from American Type Culture Collection (ATCC) (LGC standard, England) and cultured in Dubecco's Modified Eagle Medium (DMEM). The culturing medium was supplemented with 10% fetal calf serum (FCS) (Sigma-Aldrich, Dorset, UK) and 1× antimicrobial solutions (Sigma-Aldrich, Dorset, UK). Cells were cultured in an incubator with pH level of 7.3, at 95% humidity, 5% CO_2 and 37 °C.

Drugs and antibodies

Two purified chemo-drugs, paclitaxel and docetaxel purchased from Sigma-Aldrich (Dorset, UK) were dissolved and further diluted to a desired concentration. Antibodies used in protein blotting were mouse anti-human GAPDH (SC-32233) (Santa Cruz Biotechnologies Inc., CA, USA), rabbit anti-human STRN (PA5-53576) (Thermofisher, Oxford, England, UK), and rabbit anti-STRN3 (GTX65851) (GeneTex, Ely, England, UK).

Tissue cohort

Freshly frozen breast cancer tissue cohort containing both cancerous and adjacent background mammary tissues was used as previously reported (30). Written informed consent was required and obtained from patients, and a follow-up study with median follow-up period of 120 months was conducted after the surgery. The samples were collected under ethical approval (Bro Taf Health Authority; ethics approval No. 01/4303 and 01/4046).

Polymerase chain reaction (PCR) and quantitative real-time PCR (qPCR)

Gene transcripts of STRNs and the STRIPAK partners were evaluated by qPCR by employing the Amplifluor Molecular Beacon system. Reactions were prepared in a MicroAmp fast Optical 96-well plate (Fisher Scientific UK, Leicestershire, UK) using primers specific to the molecule of interest (*Supplementary Table S1*). In addition to unknown samples, reactions were prepared for a known standard that was run alongside the unknown samples on a StepOne Plus qPCR system (Fisher Scientific UK, Leicestershire, UK). Following the run, relative copy numbers of the samples were calculated as part of the systematic analysis, in accordance with the standard curve.

Breast cancer cell models

Four breast cancer cell lines, MDA-MB-231, SKBR3, MCF-7 and MDA-MB-361, representing different subtypes of breast cancer, were used to create sublines with

STRN and STRN3 knockdown by following the manufacturer's instructions. Lentiviral short hairpin RNA (shRNA) targeting human STRN (SC-37649v) and STRN3 (SG2NA) (SC-37647v) and small interfering (siRNA) targeting STRN (SC-37649) and STRN3 (SG2NA) (SC-37647) were purchased from Santa Cruz Biotechnologies Inc. Each knockdown included three sets of siRNAs. The sequences of the three sets for STRN were: set-A: Sense-CGGUGAAGAUCGAGAUACAtt and anti-sense-UGUAUCUCGAUCUUCACCGtt; set-B: Sense-CAGACUCACUAACUUAUGAtt and anti-sense-UCAUAAGUUAGUGAGUCUGtt; and set-C: Sense-CAAGGGAUAUACAAGCAUUtt and anti-sense-AAUGCUUGUAUAUCCCUUGtt. The sequences of the three sets for STRN3 were: set-A: sense-GAAUGGGCUGAACCAAUAAtt and anti-sense-UUAUUGGUUCAGCCCAUUCtt; set-B: sense-CCAGUGUAGAUCCAUAUGAtt and anti-sense-UCAUAUGGAUCUACACUGGtt; and set-C: sense-GUCUAGCAGUAGAUCCUAAtt and anti-sense: UUAGGAUCUACUGCUAGACtt. For shRNA lentiviral transduction, polybrene was used with the viral stock to transduce breast cancer cells. Puromycin was used at 2 μg/mL to select the stable knockdown cells and at 0.2 μg/mL to maintain the stability of the transfected cells.

Sodium dodecyl-sulfate polyacrylamide gel electrophoresis (SDS PAGE) and protein blotting

Proteins were extracted from cultured cells with RIPA buffer and quantified by BioRad protein quantitation kit (Bio-Rad Laboratories, Hertfordshire, UK). The samples were treated with 2× Laemmle sample buffer, boiled at 100 °C for 5 min and then loaded to 8% (for STRN and STRN3) or 10% (for GAPDH) SDS PAGE gel for electrophoresis. Semi-dry transfer system was then adopted for protein transfer from the gel onto the PVDF member which was pre-activated by methanol. Ten percent of milk was used for membrane blocking. The blots were respectively incubated with the primary antibody against STRN, STRN3 and GAPDH, followed by further exposure to the horseradish peroxidase (HRP) conjugated secondary antibody before visualized using EZ-ECL solution (Geneflow Ltd., Litchfield, UK).

Dynamic monitoring of cell behaviour with electric cell-substrate impedance sensing (ECIS)

Wild type (WT) cancer cells, the cells with STRN and STRN3 KDs, were tested using ECIS to monitor cell's biological responses following the genetic modification. Cell adhesiveness and migration was monitored according to the methods previously reported (31-33). Briefly, the respective cells were added into the 96-well microelectrode array 96W1E plate that was pre-treated for optimising electrical conductivity. The plate was mounted onto the ECIS Z-Theta unit, purchased from Applied Biophysics Inc., immediately after the cells were seeded. Cell adhesiveness was monitored for up to 6 h over all frequencies between 1,000 Hz and 64,000 Hz. For cell migration assay, the array wells were electrically wounded at 2,000 mA for 20 seconds to create cell free wounds over the gold coated electrodes. The migration pace of the cells was immediately monitored, again over the same range of frequencies for up to 20 h.

Cell matrix adhesion assays

Cell matrix adhesion assay was performed on 96-well plate that was pre-coated with Matrigel (Fisher Scientific) (5.0 μg/well). Forty thousand cells prepared in DMEM were subjected into each well followed by incubation at 37 °C with 5% CO_2. After 40 min, non-adherent cells were carefully washed with phosphate buffered saline (PBS) and the adhered cells were fixed with 4% formalin, stained with 0.5% (w/v) crystal violet, and counted under microscope at a 20× magnification. Each application was repeated 6 times and two photos were randomly taken for each well. The cell number quantification was performed by ImageJ (Version 1.53t; National Institutes of Health, Bethesda, Maryland, USA).

Patients' response to chemotherapies and evaluation

Here, we used a comprehensive public database which contain breast cancer patients with their therapeutic options recorded (34). The database took the approach of receiver operating characteristic curve (ROC), allowing classification of patients' sensitivity to a therapy. Here, the area under the curve (AUC) values and the statistical value for sensitivity to treatment were recorded. Additionally, the levels of the respective gene expression of the gene of interest were also displayed together with their statistical power (by Mann-Whitney U test).

In vitro drug sensitivity tests

Cells were seeded into 96-well plates and treated with 1:10 serial-diluted drugs. The concentrations of the drugs were

respectively chosen based on their known IC_{50} and previous studies. After 72 h, the cells were fixed with 4% formalin, stained with 0.5% crystal violet and extracted with 10% acetic acid after washing. The absorbance was measured at 595 nm using a spectrophotometer to detect their respective cell densities. The percentage drug toxicity was calculated as follows: Percentage drug toxicity = [(Absorbance in untreated well − Absorbance in drug treated well)/Absorbance in untreated well] × 100. The scatter plots of percentage toxicity versus drug concentration were plotted, and the best fit curve was used to calculate the respective IC_{50} value.

Statistical analysis

Statistical analyses were carried out using SPSS software (Version 27.0; IBM Corp., New York, USA). Groupwise comparisons were conducted by Kruskall-Wallis test and analysis of variance (ANOVA) where applicable. Integrated informatics was also tested using the Bayesian models. Pairwise comparisons were done by Mann-Whitney U test as indicated in the text. Kaplan-Meier method and log-rank test were used to run survival analysis. Univariate and multivariate analyses were conducted using Cox regression model. Classification analysis was achieved by the ROC method. P<0.05 was considered to indicate statistically significant.

Results

Expression profile of STRNs and STRIPAK complex partners in breast cancer

We quantified the transcript levels of the known STRIPAK partner molecules including all STRNs, STRIPs, calmodulin, caveolin, CCM3 (PDCD10), SIKE1, MINK1, MOB4, PPP2CA and PPP2CB, PPP2R1A and PPP2R4, MST1, TNKS1 and TNKS2 in mammary tissues of the cohort. *Tables 1,2* summarize the transcript levels of these genes in tissues and in subgroups of the patients. All three STRNs members were expressed at transcript level in mammary tissues and cancer tissues, while only STRN had a markedly higher transcript level expression in tumors than in normal tissues (P<0.01). Both of the STRNs binding proteins, calmodulin and caveolin, exhibited increased expression in the tumor tissues, yet the differences observed for calmodulin did not reach statistical significance. STRNs were not associated with Nottingham prognostic index (NPI). STRIP1, PPP2R1A and PPP2R4 were significantly elevated in high grade tumors (P<0.05) (*Table 1*). STRIP2 and MST1R were seen to significantly differ between disease free and patients with breast cancer-related incidence (*Tables 1*,*2*). The study also examined the expression levels of the STRIPAK partners in relation to ER and human epidermal growth factor receptor 2 (Her2) status and as shown in *Tables 1*,*2*, calmodulin was significantly different in ER negative and positive tumors (P<0.05). Likewise, TNKS2 and STRIP2 also significantly differ in different Her2 groups (P<0.05).

STRNs and STRIPAK, connection to clinical outcomes of patients

The expression levels of transcripts of all the STRIPAK partners were then analyzed against survival of patients by using the ROC method. Using the most favorable cutoff value generated, patients were divided into groups with high- or low-level expression and were analyzed against both overall survival (OS) and disease-free survival (DFS) by using the Kaplan-Meier method. The Cox regression model was also applied to calculate hazard ratio (HR) of each molecule against OS and DFS. As shown in *Table 3*, expression of STRIP2, calmodulin, CCM3, MINK1, MOB4, SLMAP and to a limited degree STRN3, STRN4, PPP2CA, PPP2CB, PPP2R1A had marked association with the survivals of the patients.

High-level expressions of *STRN3*, *STRN4* and *CALM* were associated with shorter OS of the patients and together they formed a poor prognostic indicator (P=0.034, HR=1.68). STRN had little impact on clinical outcomes. The other components of the core STRIPAK complex had shown a clear contrasted trend, in which high levels of *PPP2CA*, *PPP2CB* and *PPP2R1A*, but not *PPP2R4*, were seen in patients with significantly longer OS and together form a favorable prognostic indicator (P=0.034, HR=0.69). The transcript level expression of the aforementioned molecules did not show a significant correlation with DFS of the breast cancer patients (*Table 3*).

Derivation of a STRNs/STRIPAK gene signature in assessing survival of patients

The expression patterns of the shortlisted STRIPAKs were also tested using an ROC method where the patients were divided into high and low expression groups (*Figure 1A*). The cut-off value generated by the ROC curve has a significant predictive value in predicting survival outcomes of patients (AUC=0.836, P<0.001).

Table 1 Expression of STRNs and STRIPAK partners (Part 1) in mammary tissues and breast cancer tissues of Cardiff cohort

Category and subgroups	n	Median (interquartile range)									
		STRN	STRN3	STRN4	STRIP1	STRIP2	Calmodulin	PPP2CA	PPP2CB	PPP2R1A	PPP2R4
Tissue type											
Normal	33	12.05 (3.96–35.03)	0.49 (0.11–4.21)	85.3 (32.4–168.1)	4,573 (2,156–45,892)	25,857 (1,662–118,966)	3.18 (0.72–22.53)	0.3 (0.1–3.2)	0 (0–3)	1.9 (0.6–3.3)	0.00001 (0–0.00037)
Tumor	127	57 (14–288)[a]	0.75 (0.02–10.09)	84.5 (14.9–335.6)	4,156 (2,495–8,175)	10,232 (1,750–49,386)	5.7 (0.4–44.6)	0.5 (0.1–3.2)	1 (0–7)	1.58 (0.54–4.28)	0.00003 (0–0.00027)
NPI											
Good	68	63 (12–254)	0.5 (0–12.8)	78.9 (4.9–245.1)	4,192 (2,562–7,838)	12,908 (1,728–43,916)	2.9 (0.1–49.6)	0.6 (0.1–4.4)	1 (0–46)	1.52 (0.5–4.0)	0.00003 (0–0.00029)
Moderate	38	85 (15–866)	0.9 (0.1–10.2)	120.4 (32.3–606.9)	4,553 (2,440–9,838)	4,761 (120–109,529)	12.1 (1.8–45.4)	0.22 (0.04–7.37)	0.9 (0.2–3.1)	1.862 (0.409–4.352)	0.00005 (0–0.00032)
Poor	16	49.7 (6.6–248.8)	1.07 (0.03–13.21)	91.8 (33.5–331.8)	3,326 (1,906–15,825)	9,787 (768–213,921)	2.62 (0.25–17.95)	0.69 (0.18–1.35)	0 (0–1)	1.869 (0.657–3.836)	0.0001 (0–0.0002)
Grade											
Grade 1	24	25 (1–629)	0.16 (0–10.13)	50 (2–585)	3,209 (2,210–4,545)	15,580 (2,221–94,997)	2 (0–35)	0.3 (0.1–4.5)	1.3 (0.2–2.7)	0.597 (0.121–2.084)	0.00002 (0–0.00018)
Grade 2	43	94 (26–557)	0.5 (0.1–14.9)	102 (10–399)	3,708 (1,673–7,023)	9,526 (411–47,310)	2.3 (0.1–52.5)	0.32 (0.04–1.68)	1 (0–14)	2.101 (1.05–5.55)[b]	0.00002 (0–0.00014)[d]
Grade 3	58	49.7 (7.1–209.8)	1.1 (0.2–7.5)	84.8 (35.3–238.2)	6,101 (2,909–16,558)[b]	8,105 (1,854–83,647)	11.1 (1.8–44.6)	0.82 (0.11–5.22)	1 (0–11)	1.37 (0.52–4.32)	0.00007 (0–0.00034) [d]
Clinical outcome											
Disease free	90	49 (7–455)	0.8 (0–12.5)	96.8 (14.7–357.8)	3,914 (2,577–7,390)	12,543 (2,031–68,358)	6.3 (0.4–46.2)	0.5 (0.1–2.1)	1 (0–6)	1.49 (0.53–4.02)	0.00002 (0–0.00022)
With metastasis	7	73.5 (25.1–212.5)	0.83 (0.16–7.77)	85.0 (55.2–125.2)	2,868 (1,684–6,967)	199 (31–1,972)[c]	5.4 (0–55.9)	1.8 (0.1–8.2)	1.4 (0.4–170.6)	1.88 (1.14–9.62)	0.00042 (0.00001–0.00067)
Died of BrCa	16	149 (4–667)	0.89 (0.04–7.56)	99.9 (11.6–463.4)	7,150 (2,466–19,400)	8,148 (701–32,499)	10.2 (0.8–40.7)	0.18 (0.06–2.17)	1 (0–8)	2.6 (0.5–7.7)	0.00008 (0–0.00014)
All incidence	28	80.2 (32.1–250.7)	0.77 (0.04–6.43)	81.2 (28.3–270.2)	5,685 (1,811–9,074)	2,537 (278–29,621)	7.5 (0.4–44.6)	0.66 (0.08–2.87)	1.4 (0.2–8.4)	2.12 (1.14–7.73)	0.00008 (0–0.00031)
Nodal status											
Positive	54	55 (15–554)	1.4 (0.1–10.2)	119.8 (33.2–420.6)	4,545 (2,483–10,050)	8,127 (701–119,800)	9.7 (0.9–43.2)	0.42 (0.08–2.27)	1 (0–2)	1.869 (0.518–4.237)	0.00005 (0–0.00033)
Negative	68	63 (12–254)	0.5 (0–12.8)	78.9 (4.9–245.4)	4,192 (2,562–7,838)	12,908 (1,728–43,916)	2.9 (0.1–49.6)	0.6 (0.1–4.4)	1 (0–46)	1.52 (0.52–4.23)	0.00003 (0–0.00029)
ER status											
Negative	75	57.4 (14.3–287.7)	1.0 (0–10.7)	85.2 (19.6–305.2)	3,337 (2,483–6,189)	14,070 (1,868–47,039)	11.1 (1.5–51.3)	0.5 (0.1–4.2)	1 (0–8)	1.585 (0.525–3.836)	0.00004 (0–0.00031)
Positive	38	59 (11–2,129)	0.5 (0–6.5)	78.9 (3.9–493.7)	5,055 (2,528–8,209)	6,278 (793–55,289)	2.1 (0–17.9)[d]	0.55 (0.07–3.81)	1 (0–6)	2.10 (0.45–6.42)	0.00005 (0–0.00014)
Her2											
Negative	57	52 (7–586)	1.1 (0.1–15.1)	102.1 (16.4–398.5)	4,545 (2,184–8,001)	33,053 (7,107–101,396)	5.3 (0.5–29.6)	0.8 (0.2–3.3)	1 (0–6)	1.49 (0.48–3.84)	0.00004 (0–0.00027)
Positive	55	81 (29–254)	0.75 (0.02–7.14)	84.5 (13.8–311.9)	3,632 (2,355–8,786)	5,958 (806–30,208)[e]	12.0 (0.4–49.1)	0.33 (0.08–3.23)	1 (0–8)	1.71 (0.50–4.51)	0.00002 (0–0.00032)

STRIPAK, striatin-interacting phosphatases and kinases; NPI, Nottingham prognostic index; BrCa, breast cancer; ER, estrogen receptor; Her2, human epidermal growth factor receptor 2; STRN, striatin; STRIP1, striatin interacting proteins 1; PP2A, protein phosphatase 2A; PPP2R1A, PP2A regulatory subunit A. Mann-Whitney U tests were conducted, and statistical significance was reached by comparing between groups. [a], *vs.* normal, P<0.05; [b], *vs.* Grade 1, P<0.05; [c], *vs.* disease free, P<0.05; [d], *vs.* ER negative, P<0.05; [e], *vs.* Her2 negative, P<0.05.

Integration of core molecules of the STRIPAK complex constitutes a highly significant prognostic indicator for OS [P<0.001, HR=2.04, 95% confidence interval (CI): 1.36–3.07] and DFS (P=0.003, HR=1.40, 95% CI: 1.12–1.75) (*Figure 1*). To evaluate the signature independency in predicting OS, we carried out multivariate analysis together with other clinical and indeed hormone receptor-based subtype analysis. As shown in *Table 4*, the

Table 2 Expression of STRNs and STRIPAK partners (Part 2) in mammary tissues and breast cancer tissues of Cardiff cohort

Category and subgroups	n	Median (interquartile range)									
		CCM3	MINK1	MOB4	SIKE1	SLMAP	MST1 (HGFL)	MST1R (RON)	Caveolin	TNKS1	TNKS2
Tissue type											
Normal	33	6,790 (3,773–15,861)	5,948 (2,561–9,834)	20,235 (9,388–25,369)	2,153 (499–3,581)	4,453 (2,161–9,633)	7 (0–412)	0 (0–179)	0.164 (0.047–0.363)	2.26 (0.87–6.03)	0.01 (0–0.73)
Tumor	127	6,183 (1,734–23,717)	5,525 (1,996–17,477)	19,852 (7,196–38,318)	1,995 (971–4,135)	3,243 (1,378–17,215)	2 (0–349)	0 (0–1,488)	0.45 (0.09–2.49)	5.8 (0.5–22.7)	0.01 (0–3.22)
NPI											
Good	68	6,832 (1,827–23,843)	5,343 (1,655–16,941)	18,779 (7,947–33,941)	1,907 (984–3,997)	2,904 (1,252–16,639)	0 (0–466)	0 (0–787)	0.358 (0.078–2.140)	1.93 (0.31–16.92)	0.09 (0–4.55)
Moderate	38	7,508 (1,284–34,305)	6,328 (2,014–28,532)	19,848 (4,955–41,073)	2,499 (1,338–5,834)	4,575 (1,445–17,335)	3 (0–487)	0 (0–160)[a]	0.68 (0.12–2.53)	7.9 (1.0–26.7)	0 (0–0.9)
Poor	16	4,619 (2,687–24,503)	5,678 (2,431–23,419)	31,648 (16,480–42,687)	948 (463–2,884)	9,459 (3,121–44,016)	1 (0–249)	350 (0–41,341)[b]	0.78 (0.12–7.38)	12 (1–44)	0 (0–2.57)
Grade											
Grade 1	24	3,688 (1,613–13,758)	4,476 (1,148–13,647)	14,373 (3,902–25,883)	2,023 (1,224–5,861)	3,243 (1,749–25,592)	0 (0–135)	0 (0–1,211)	1.3 (0.1–2.7)	3.6 (0.2–9.4)	0 (0–2.61)
Grade 2	43	5,499 (1,048–20,152)	5,905 (1,348–17,857)	18,203 (5,514–33,671)	3,063 (1,569–4,265)	2,603 (882–9,366)	9 (0–737)	0 (0–76)	0.597 (0.093–2.691)	2.57 (0.32–17.71)	0.14 (0–4.61)
Grade 3	58	7,049 (2,832–28,673)	5,525 (2,106–21,790)	26,244 (13,390–40,611)	1,601 (553–2,593)	6,690 (1,772–36,975)	0 (0–328)	4 (0–9,011)	0.37 (0.08–1.50)	9.9 (0.9–36.0)	0 (0–2.95)
Clinical outcome											
Disease free	90	5,741 (1,892–24,631)	5,658 (2,205–16,122)	20,591 (7,196–38,318)	2,257 (1,295–3,747)	2,805 (1,279–15,751)	14 (0–494)	0 (0–212)	0.47 (0.11–2.55)	6.2 (0.5–17.7)	0.01 (0–3.55)
With metastasis	7	3,607 (734–4,230)	4,353 (2,673–5,150)	22,548 (8,688–37,321)	2,800 (592–5,278)	2,802 (882–3,037)	0 (0–777)	0 (0–101)	0.05 (0.01–0.78)	15.2 (3.3–64.2)	0.002 (0–0.183)
Died of BrCa	16	11,445 (3,734–47,878)	15,408 (1,529–28,364)	35,484 (18,815–41,867)	1,086 (401–5,153)	7,772 (1,916–44,016)	0 (0–51)	9,020 (0–41,341)	0.33 (0.03–1.83)	11 (1–44)	0.06 (0–18.82)
All incidence	28	6,959 (1,245–24,352)	4,379 (1,909–26,160)	31,648 (10,839–41,073)	1,623 (414–4,377)	6,883 (1,836–31,760)	0 (0–51)	39 (0–17,005)[c]	0.23 (0.03–1.83)	11.9 (0.9–64.2)	0.01 (0–2.57)
Nodal status											
Positive	54	6,652 (1,875–24,807)	5,905 (2,303–26,199)	27,954 (8,118–41,469)	2,393 (1,290–4,283)	6,883 (1,567–29,843)	2 (0–320)	1 (0–4,320)	0.68 (0.12–2.63)	9.2 (0.9–31.0)	0 (0–1.18)
Negative	68	6,832 (1,827–23,843)	5,343 (1,655–16,941)	18,779 (7,947–33,941)	1,907 (984–3,997)	2,904 (1,252–16,639)	0 (0–466)	0 (0–787)	0.358 (0.078–2.141)	1.93 (0.31–16.92)	0.09 (0–4.55)
ER status											
Negative	75	4,667 (1,908–20,436)	5,736 (2,495–16,532)	25,332 (14,048–37,111)	1,823 (1,290–3,090)	2,853 (1,395–14,034)	14 (0–698)	1 (0–2,315)	0.31 (0.07–1.98)	5.14 (0.48–18.42)	0.01 (0–3.26)
Positive	38	7,265 (1,428–24,809)	4,405 (765–21,412)	14,850 (5,222–40,614)	2,084 (616–5,301)	4,351 (1,306–27,238)	0 (0–70)	0 (0–1,005)	0.777 (0.173–2.534)	5.3 (0.8–23.6)	0.01 (0–3.68)
Her2											
Negative	57	4,817 (1,899–24,173)	6,116 (3,052–16,218)	20,591 (11,843–36,248)	2,522 (984–5,112)	3,690 (1,388–17,456)	9 (0–447)	0 (0–1,312)	0.75 (0.11–2.17)	1.5 (0.3–18.4)	0.01 (0–3.89)
Positive	55	7,472 (1,657–25,436)	4,379 (1,491–20,523)	19,852 (6,181–39,955)	1,826 (744–3,734)	3,093 (1,333–19,952)	0 (0–296)	0 (0–2,165)	0.36 (0.07–1.83)	8.3 (1.3–39.2)	0 (0–3.36)[d]

STRIPAK, striatin-interacting phosphatases and kinases; NPI, Nottingham prognostic index; BrCa, breast cancer; ER, estrogen receptor; Her2, human epidermal growth factor receptor 2; CCM3, cerebral cavernous malformations 3; MINK1, misshapen like kinase 1; MOB4, Mps one binder kinase activator family member 4; SIKE1, suppressor of IKK epsilon 1; MST1, macrophage stimulating 1; TNKS, tankyrase; Mann-Whitney U tests were conducted and statistical significance was reached by comparing between the groups. [a], *vs.* good prognosis, P<0.05; [b], *vs.* moderate prognosis, P<0.05; [c], *vs.* disease free, P<0.05; [d], *vs.* Her2 negative, P<0.05.

STRIPAK signature presents a significant prognostic value (P<0.001) independent from other clinical factors and hormone receptor status of patients.

The prognostic value in patients' OS was additionally tested using the Bayesian model that has returned a Bayes factor at 2.1×10^{-4} with a mode factor at 3.22, strongly

Table 3 STRIPAK and patients' OS and DFS, Cardiff data by Cox regression

Variables	OS		DFS	
	P	HR	P	HR
STRN	0.434	1.804 (0.411–7.918)	0.260	2.306 (0.539–9.871)
STRN3	0.178	2.031 (0.724–5.700)	0.384	1.465 (0.621–3.456)
STRN4	0.196	3.789 (0.504–28.492)	0.248	2.352 (0.551–10.038)
STRIP1	0.053	3.018 (0.984–9.254)	0.249	1.853 (0.649–5.292)
STRIP2	0.014	4.388 (1.349–14.267)	0.265	1.781 (0.646–4.913)
Calmodulin	0.019	4.384 (1.269–15.149)	0.055	2.489 (0.981–6.316)
PPP2CA	0.063	0.414 (0.163–1.050)	0.069	0.468 (0.206–1.061)
PPP2CB	0.110	0.471 (0.187–1.186)	0.105	0.509 (0.224–1.153)
PPP2R1A	0.079	0.436 (0.173–1.100)	0.073	0.473 (0.208–1.073)
PPP2R4	0.590	1.292 (0.509–3.278)	0.752	1.141 (0.503–2.589)
CCM3	0.032	4.003 (1.128–14.205)	0.488	1.381 (0.555–3.437)
MINK1	0.011	3.749 (1.356–10.361)	0.146	2.053 (0.779–5.410)
MOB4	0.010	4.598 (1.441–14.676)	0.075	2.460 (0.915–6.613)
SIKE1	0.115	3.056 (0.763–12.246)	0.136	2.467 (0.752–8.086)
SLMAP	0.035	3.496 (1.093–11.176)	0.178	2.033 (0.723–5.714)
MST1 (HGFL)	0.441	0.646 (0.213–1.964)	0.358	0.628 (0.233–1.693)
MST1R (RON)	0.415	1.473 (0.581–3.735)	0.285	1.569 (0.687–3.580)
Caveolin	0.674	0.816 (0.315–2.110)	0.303	0.648 (0.283–1.481)
TNKS1	0.093	5.666 (0.748–42.940)	0.054	7.253 (0.970–54.222)
TNKS2	0.261	1.854 (0.633–5.431)	0.692	1.194 (0.497–2.870)

STRIPAK, striatins interacting phosphatase and kinase; OS, overall survival; DFS, disease-free survival; STRN, striatin; STRIP, striatin interacting protein; CCM3, cerebral cavernous malformations 3; MINK1, misshapen like kinase 1; MOB4, Mps one binder kinase activator family member 4; SIKE1, suppressor of IKK epsilon 1; MST1, macrophage stimulating 1; TNKS, tankyrase; HR, hazard ratio.

suggesting that the signature has a strong value to predict patients' survival outcomes.

The signature has also significantly correlated with DFS (P=0.003) (*Figure 1C*), supported by the independent Bayesian model with Bayes factor at 0.26. We further stratified the patients with conventional biomarkers, namely ER and Her2 status. As shown in *Figure 1*, the signature identified those with worst outcomes who had ER(−), Her2(+) and most strongly ER(−)/Her2(+) tumors. It is also noteworthy that the signature has not improve the prediction of outcome in triple-negative breast cancer (TNBC) (*Figure 1F2*).

STRNs and STRIPAK and patients' response to drug treatment, using The Cancer Genome Atlas (TCGA)/ROC plot dataset

To understand if and how STRNs and other STRIPAK partner may influence patients' response to chemotherapies, we explore the TCGA dataset that had information on tumor's pathological response and patient's response evaluated by the 5-year relapse-free survival (RFS). When assessed for the pathological responses (*Table 5*), it was shown that when STRN3, CCM3, MOB4A, PPP2CA and PPP2CB levels were high, patients were significantly responsive to chemotherapies. Instead, high levels of STRN4, PPP2R1A and MST1 expression are associated with a significant increase in the chance of drug resistance. In a similar pattern when assessed for the 5-year RFS response as shown in *Table 6*, patients with tumors that express high levels of STRN3, STRIP2, PPP2CA and PPP2CB were more sensitive to chemotherapies. In contrast, those with high levels of SIKE1, MOB4 and MST1 were more resistant to chemotherapies.

STRN3 is the key scaffold protein for the STRIPAK complex, of which other partner proteins dock on the duplex protein structure formed by STRN3. To assess if

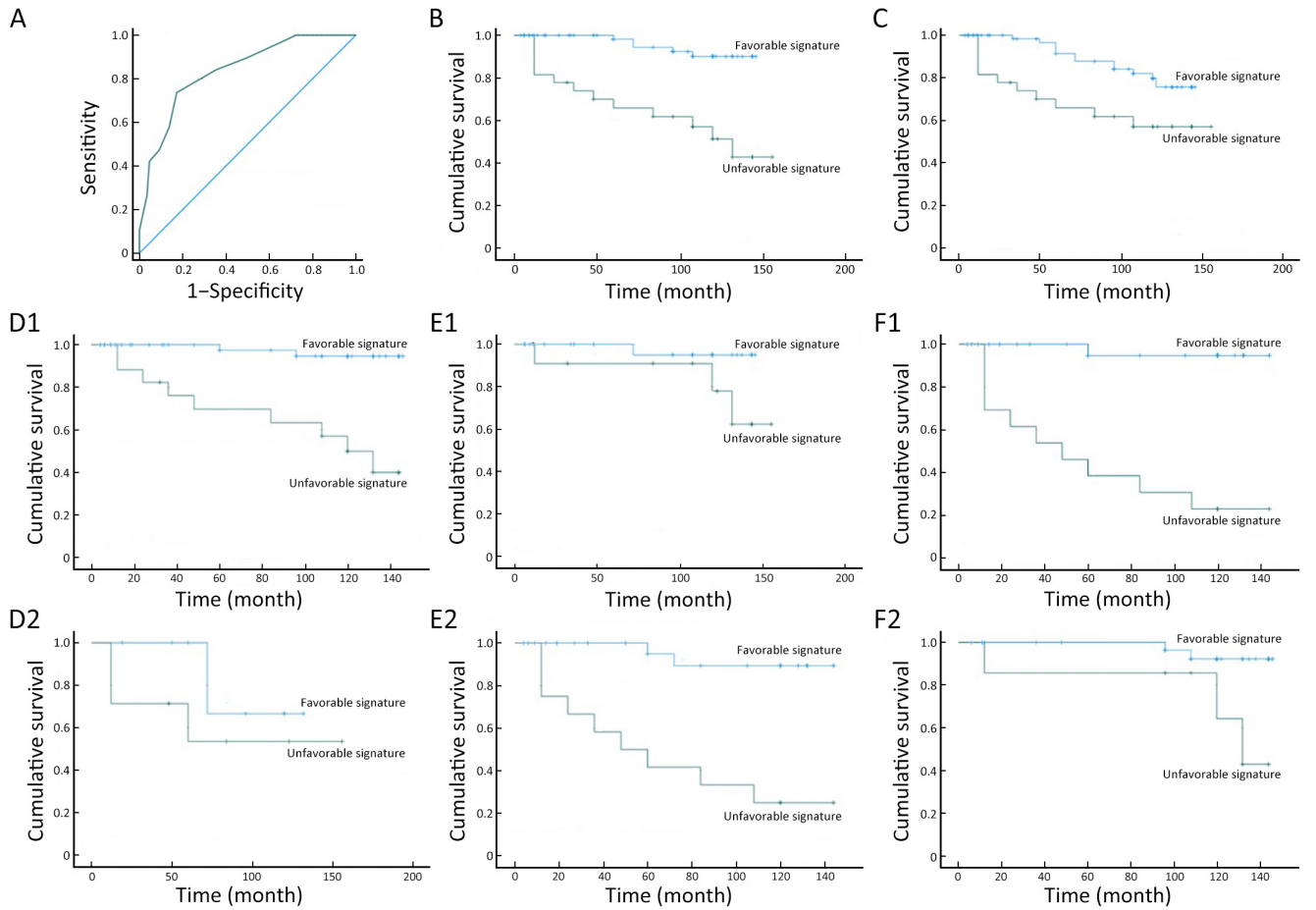

Figure 1 Integrated STRN and other core STRIPK members and prediction of patient survival. (A) The expression pattern of the shortlist STRIPAKs is tested using ROC method. There is a significant predictive value in predicting OS (AUC=0.836, P<0.001); (B,C) Patients were then stratified into two groups based on their expression pattern of the signature. The stratification showed a highly significant value in predicting OS (P<0.001) (B) and DFS (P=0.003) (C); (D–F) The signature identified those patients who had worst outcomes in ER(−) tumors (P<0.001) (D1), Her2(+) tumors (P<0.001) (E2) and more profoundly in ER(−)/Her2(+) tumors (P<0.001) (F1); whereas it had little additional value for ER(+) tumors (P=0.292) (D2), Her2(−) tumors (P=0.088) (E1) and TNBC (P=0.017) (F2). OS, overall survival; DFS, disease-free survival; ER, estrogen receptor; Her2, human epidermal growth factor receptor 2; −, negative; +, positive; TNBC, triple-negative breast cancer.

expression of STRN3 itself has an impact on drug responses, we further explored the link between STRN3 in the subtype of breast cancer by considering the hormone receptor status, again by the pathological and 5-year RFS response (*Table 7*). In ER-positive and Her2-negative tumors, higher STRN3 levels are significantly associated with elevated chemosensitivity in both the tumors' pathological and patients' 5-year RFS responses. This is additionally reflected very well in patients with ER(+)/Her2(−) tumors. In contrast, high levels of STRN3 in Her2(+) tumors and Her2(+)/ER(−) subtypes are associated with increased resistance to chemotherapies.

Creation of STRN knockdown and STRN3 knockdown models from breast cancer cell lines with different receptor status

In the light of the findings that STRIPAK complex molecules had a significant bearing on the clinical progression and in particular on the clinical outcome of the patients, as well as patient's response to drug treatment, we created a set of breast cancer cell models to further investigate this link. We have chosen 4 breast cancer cell lines, each representing a subtype of breast cancer with different hormone receptor status. They were ER(+)/Her2(−) MCF-7, ER(−)/Her2(+) SKBR3,

Table 4 Univariate and multivariate analysis of STRIPAK signature and clinical factors against OS (Cox regression)

Factors tested	Univariate		Multivariate	
	HR (95% CI)	P	HR (95% CI)	P
STRN/STRIPAK signature	1.203 (1.095–1.322)	<0.001	1.284 (1.127–1.463)	<0.001
Clinical factors				
NPI	2.874 (1.579–5.230)	0.001	2.582 (0.654–10.198)	0.176
Grade	1.121 (0.821–1.530)	0.472	1.503 (0.756–2.985)	0.245
Staging	1.269 (0.897–1.796)	0.178	1.331 (0.800–2.215)	0.271
Nodal status	4.688 (1.575–14.557)	0.006	0.602 (0.060–6.006)	0.666
ER	2.375 (0.818–6.896)	0.112	2.647 (0.785–8.930)	0.117
Her2	3.181 (1.010–10.022)	0.048	4.682 (1.274–17.208)	0.020
Receptor subtypes				
TNBC	2.417 (0.858–6.810)	0.095	0.383 (0.042–3.513)	0.396
ER(+)/Her2(−)	2.631 (0.981–7.059)	0.055	2.119 (0.274–16.358)	0.472
ER(−)/Her2(+)	2.871 (1.110–7.247)	0.030	4.537 (0.592–34.756)	0.145
ER(+)/Her2(+)	2.123 (1.202–3.749)	0.010	1.435 (0.474–4.346)	0.522

STRIPAK, striatins interacting phosphatase and kinase; OS, overall survival; STRN, striatin; NPI, Nottingham prognostic index; ER, estrogen receptor; Her2, human epidermal growth factor receptor 2; TNBC, triple-negative breast cancer; HR, hazard ratio; 95% CI, 95% confidence interval.

ER(−)/Her2(−) MDA-MB-231 and ER(+)/Her2(+) MDA-MB-361. The knockdown efficiency of STRN and STRN3 is illustrated in *Figure 2A*. We had also tested the protein expression profile of the two molecules before and after knockdown in the breast cancer cell lines by Western blot (*Figure 2B*). The cell models created were subsequently used for *in vitro* experiments.

Effects of STRN and STRN3 knock down on cell behaviour in breast cancer cells with different receptor status

All of the four cell lines were chosen for ECIS application. By varying the frequency of the applied current, ECIS could distinguish intercellular resistance and cell to matrix resistance. The resistance measured at lower frequency could provide more accurate data regarding the dynamic change of cell-cell contact, as low frequency current is more likely to go under and between the cell gaps. The firmer the cell junction, the greater the resistance at lower frequency. In contrast, higher frequency current is more optimal for measuring cell-matrix interactions and thereby the cell attachment. The resistance increases along with more cells adhered to the 96-well plate base. Meanwhile, the rate of cell adhesion could be reflected by the steepness of the line.

In the present study, the attachment and spreading of these cells with and without STRN or STRN3 knockdown were real-time monitored. As we can see from *Figure 3* which represented the cell behavior changes of MDA-MB-231 cells, the WT cells had the lowest resistance throughout both adhesion and wound healing period compared with the other two MDA-MB-231-KD cell models. The same pattern across all frequencies was seen in the corresponded 3D graphs (*Figure 3*). The lower the frequency, the higher resistance for the two MDA-MB-231-KD cell lines and differences with the WT cell. The results indicated the reduced expression of STRNs, especially STRN3, would facilitate cell adhesion and migration in TNBC cells.

MDA-MB-361 with and without STRNs KD responded in an opposite way during cell attachment and wound healing compared with MDA-MB-231 (*Figure 4*). The behavior differences between STRN-KD and STRN3-KD cells were not obvious at 4,000 Hz, yet they both displayed greater cell-matrix adhesiveness and reduced spreading during wounding process when compared with WT cells. The reduced migration after STRNs member KD was also seen in MCF-7 cells, another ER(+) cell line, of which the resistance during wound healing was greatly suppressed especially with STRN3-KD (*Figure 5*). A similar trend was also observed during the attachment process in a less striking way that the MCF WT cells exhibited stronger adhesiveness, although the difference was not highly

Table 5 Patient's drug response, tumor pathological responses to chemotherapies*

Molecule and response status	n	Transcript expression level		ROC	
		Median (min–max)	P	AUC	P
STRN3			<0.001	0.565	<0.001
Responders	532	428 (4–2,480)			
Non-responders	1,100	342 (6–3,394)			
STRN4			<0.001	0.631	<0.001
Responders	532	191 (9–1,068)			
Non-responders	1,100	314 (6–1,460)			
STRIP1 (FAM40A)			0.340	0.529	0.180
Responders	119	464 (105–1,057)			
Non-responders	388	436 (50–1,339)			
STRIP2 (FAM40B)			0.300	0.531	0.150
Responders	119	54 (2–819)			
Non-responders	388	47 (0–855)			
Calmodulin			0.150	0.522	0.076
Responders	532	1,696 (52–7,615)			
Non-responders	1,100	1,547 (23–10,294)			
SIKE1			0.170	0.542	0.073
Responders	119	452 (24–1,382)			
Non-responders	388	504 (5–4,356)			
MINK1			0.530	0.510	0.260
Responders	532	1,062 (285–9,626)			
Non-responders	1,100	1,098 (72–14,670)			
CCM3 (PDCD10)			<0.001	0.588	<0.001
Responders	532	3,443 (7–13,811)			
Non-responders	1,100	2,876 (15–13,752)			
MOB4B (MOBKL1B)			0.850	0.503	0.420
Responders	532	1,287 (48–5,356)			
Non-responders	1,100	1,270 (21–6,644)			
MOB4A (MOBKL1A)			0.060	0.557	0.031
Responders	119	1,255 (163–3,290)			
Non-responders	388	1,097 (70–5,515)			
PPP2R1A			<0.001	0.619	<0.001
Responders	532	538 (25–3,238)			
Non-responders	1,100	1,150 (35–4,831)			
PPP2CA			0.016	0.537	0.008
Responders	532	2,268 (241–5,931)			
Non-responders	1,100	2,031 (87–6,764)			
PPP2CB			<0.001	0.558	<0.001
Responders	532	2,990 (195–10,822)			
Non-responders	1,100	1,510 (25–12,568)			
MST1R			<0.001	0.601	<0.001
Responders	532	265 (10–1,611)			

Table 5 (*continued*)

Table 5 (*continued*)

Molecule and response status	n	Transcript expression level		ROC	
		Median (min–max)	P	AUC	P
Non-responders	1,100	342 (19–1,774)			
PPP2R4			<0.001	0.645	<0.001
Responders	532	659 (150–3,102)			
Non-responders	1,100	904 (99–5,432)			
Caveolin			<0.001	0.575	<0.001
Responders	532	1,542 (12–24,193)			
Non-responders	1,100	974 (3–22,206)			
TNKS2			<0.001	0.630	<0.001
Responders	532	866 (3–4,463)			
Non-responders	1,100	532 (9–2,929)			

STRN, striatin; STRIP, striatin interacting protein; SIKE1, suppressor of IKK epsilon 1; MINK1, misshapen like kinase 1; CCM3, cerebral cavernous malformations 3; MOB4, Mps one binder kinase activator family member 4; MST1, macrophage stimulating 1; TNKS, tankyrase; ROC, receiver operating characteristic; AUC, area under the curve. *, from ROCplot.com (34).

significant (*Figure 5*).

Contrary to what we observed in ER(+)/Her2(−) cell, SKBR3 with opposite receptor status exhibited a different cell response during adhesion and migration (*Figure 6*). As an ER(−)/Her2(+) cell line, STRN and STRN3 significantly facilitated both processes with STRN3 contributing more to attachment and STRN to cell motility. Moreover, the cell-matrix and cell-cell interactions were higher in the STRNs KD groups during adhesion and migration, respectively, as shown in the 3D graphs, which reflect resistance at different frequencies.

We have additionally validated the finding from the automated ECIS analyses on the cell models by employing a traditional cell-matrix adhesion assay. As shown in *Figure 3*, the MDA-MB-231 STRN-KD and STRN3-KD cells showed significantly increased number of adhered cells at the time of fixation compared with the control MDA-MB-231 WT cells. This result has aligned with our finding reflected from ECIS application. A similar but less pronounced trend was observed in the MDA-MB-361 cell line, with the KD cells exhibiting greater adhesion ability to the gel base (*Figure 7*).

Expression of STRNs in breast cancer cell response to chemo-drugs, determined by in vitro study

The four breast cancer cell lines were subsequently tested with their responses to chemotherapy drugs following confirmation of knockdown of STRN and STRN3 (*Table 8*). Under the *in vitro* condition used, MDA-MB-231 (triple negative) cells with reduced STRN and STRN3 expression exhibited higher IC_{50} to both chemo-drugs, revealing an increase in drug resistance after knocking down STRN or STRN3 compared with WT cells. No difference in drug resistance was observed between the WT MDA-MB-361 and the corresponding STRN3-KD cells, while the cells with STRN-KD were more responsive to docetaxel. Whilst the lack in expression of STRN3 suppressed the MCF-7 cells' sensitivity to docetaxel, it decreased the IC_{50} in SKBR3 cells with STRN3-KD, elevating the toxicity of docetaxel to SKBR3/STRN3-KD cells. In terms of the drug responses of MCF-7 and SKBR3 to paclitaxel, the cells that were lessen in STRN level had shown better response to the drug therapy compared with the respective WT and STRN3-KD cells.

Discussion

In the present report, we have shown for the first time the full profile of STRNs and their binding-partner proteins in STRIPAK complex in clinical breast cancer, as well as their relationships to breast cancer patients' responses to drug treatment and clinical outcomes. The study also examined the impact of targeting the backbone of the STRIPAK, namely STRNs, in cell models on cell behavior and responsiveness to chemo-drugs in conjunction with the clinical data on the impact of STRIPAK members' transcript levels on drug responses.

The STRIPAK complex, with STRNs acting as the scaffolding unit, contains both kinases and phosphatases. STRIPAKs play critical roles in process of protein phosphorylation and dephosphorylation, serving as important regulators of multiple signaling pathways

Table 6 Patient's drug response, 5-year RFS response to chemotherapies*

Molecule and response status	n	Transcript expression level		ROC	
		Median (min–max)	P	AUC	P
STRN3			<0.001	0.587	<0.001
Responders	256	451 (15–2,923)			
Non-responders	220	362 (32–2,391)			
STRN4			0.420	0.521	0.210
Responders	256	424 (107–1,411)			
Non-responders	220	393 (101–1,785)			
STRIP1 (FAM40A)			0.780	0.514	0.390
Responders	115	444 (141–806)			
Non-responders	48	411 (243–744)			
STRIP2 (FAM40B)			0.074	0.589	0.042
Responders	115	46 (1–1,234)			
Non-responders	48	34 (2–180)			
Calmodulin			0.200	0.534	0.097
Responders	256	1,759 (488–6,555)			
Non-responders	220	1,660 (463–5,411)			
SIKE1			0.003	0.646	0.001
Responders	115	393 (5–1,225)			
Non-responders	48	500 (38–1,027)			
MINK1			0.300	0.528	0.150
Responders	256	1,169 (267–5,696)			
Non-responders	220	1,266 (312–3,739)			
CCM3 (PDCD10)			0.730	0.509	0.370
Responders	256	2,982 (428–12,107)			
Non-responders	220	2,990 (570–11,370)			
MOB4B (MOBKL1B)			0.091	0.545	0.044
Responders	532	1,160 (347–3,723)			
Non-responders	256	1,268 (431–3,500)			
MOB4A (MOBKL1A)			0.810	0.512	0.400
Responders	220	596 (116–3,018)			
Non-responders	48	563 (248–1,404)			
PPP2R1A			0.800	0.507	0.400
Responders	256	1,370 (348–3,557)			
Non-responders	220	1,334 (420–3,058)			
PPP2CA			<0.001	0.598	<0.001
Responders	256	2,394 (665–5,597)			
Non-responders	220	1,994 (241–5,705)			
PPP2CB			0.003	0.579	0.001
Responders	256	3,030 (339–11,837)			
Non-responders	220	2,577 (785–10,412)			
MST1R			0.014	0.565	0.007

Table 6 (*continued*)

Table 6 (*continued*)

Molecule and response status	n	Transcript expression level		ROC	
		Median (min–max)	P	AUC	P
Responders	256	360 (16–2,343)			
Non-responders	220	418 (25–1,351)			
PPP2R4			0.090	0.545	0.044
Responders	256	1,106 (299–3,980)			
Non-responders	220	1,018 (317–3,727)			
Caveolin			0.210	0.533	0.110
Responders	256	1,097 (15–8,858)			
Non-responders	220	16 (12,599)			
TNKS2			0.007	0.572	0.003
Responders	256	798 (65–2,913)			
Non-responders	220	640 (114–2,098)			

RFS, relapse-free survival; STRN, striatin; STRIP, striatin interacting protein; SIKE1, suppressor of IKK epsilon 1; MINK1, misshapen like kinase 1; CCM3, cerebral cavernous malformations 3; MOB4, Mps one binder kinase activator family member 4; MST1, macrophage stimulating 1; TNKS, tankyrase; ROC, receiver operating characteristic; AUC, area under the curve. *, from ROCplot.com (34).

Table 7 STRN3 transcript expression level and patients' response to chemotherapies in subtypes of breast cancer (*by Mann-Whitney U test)

Hormone receptor and subtypes	Pathological response				5-year RFS response			
	Response status	n	Median (min–max)	P	Response status	n	Median (min–max)	P
ER status								
ER(–)	Responders	279	338 (15–2,480)	0.700	Responders	115	446 (15–2,014)	0.120
	Non-responders	387	351 (32–3,394)		Non-responders	111	360 (32–2,391)	
ER(+)	Responders	253	517 (4–1,927)	<0.001	Responders	141	454 (16–2,923)	0.003
	Non-responders	713	338 (6–3,160)		Non-responders	109	363 (85–1,092)	
Her2 status								
Her2(–)	Responders	389	505 (4–2,480)	<0.001	Responders	183	409 (15–1,610)	0.004
	Non-responders	890	336 (6–3,160)		Non-responders	173	331 (32–1,104)	
Her2(+)	Responders	143	301 (64–2,190)	0.001	Responders	73	593 (133–2,923)	0.310
	Non-responders	210	404 (18–3,394)		Non-responders	47	549 (153–2,391)	
ER/Her2 status subtypes								
ER(–)/Her2(+)	Responders	83	304 (64–2,190)	0.003	Responders	35	655 (133–2,014)	0.690
	Non-responders	110	419 (106–3,394)		Non-responders	26	580 (161–2,391)	
ER(+)/Her2(–)	Responders	193	720 (4–1,927)	<0.001	Responders	103	409 (16–1,349)	0.017
	Non-responders	613	334 (6–3,160)		Non-responders	88	336 (85–1,092)	
ER(+)/Her2(+)	Responders	60	288 (76–1,564)	0.053	Responders	38	579 (216–2,923)	0.100
	Non-responders	100	364 (18–2,645)		Non-responders	21	512 (153–957)	
TNBC	Responders	196	428 (15–2,480)	0.140	Responders	80	413 (15–1,610)	0.130
	Non-responders	277	339 (32–2,180)		Non-responders	84	328 (32–1,104)	

STRN, striatin; RFS, relapse-free survival; ER, estrogen receptor; Her2, human epidermal growth factor receptor 2; TNBC, triple-negative breast cancer; *, from ROCplot.com (34).

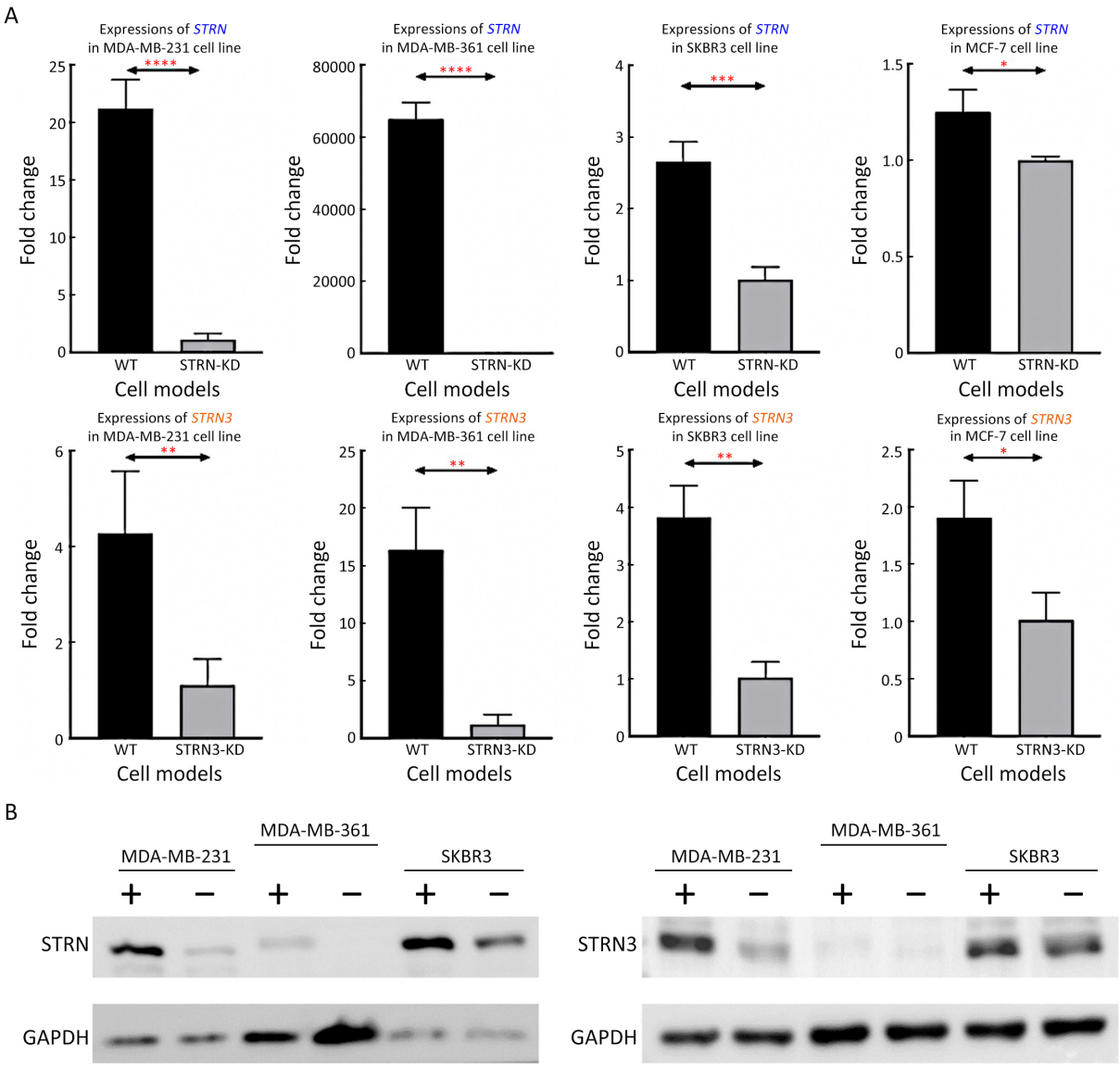

Figure 2 Expression of STRN and STRN3 in breast cancer cell lines. (A) qPCR confirmation of KDs. Semi-quantitative analysis of the relative gene expression of *STRN* and *STRN3* in the four breast cancer cell lines, MDA-MB-231, MDA-MB-361, SKBR3, MCF-7. The fold change was acquired by $2^{-\Delta\Delta Ct}$ which is a formula used to calculate the relative fold change expression when performing qPCR. Unpaired *t*-test was performed to statistically analyze the degree of KDs. *, P<0.05; **, P<0.01; ***, P<0.001; ****, P<0.0001; (B) Western blot shows the STRN and STRN3's protein expression, respectively in WT(+) and KD(−) MDA-MB-231, MDA-MB-361 and SKBR3 cell lines. The corresponded protein expression of the housekeeping gene, GAPDH, in each cell model is also demonstrated. qPCR, quantitative real-time polymerase chain reaction; WT, wild type; KD, knockdown.

involved in cell growth, differentiation, proliferation and apoptosis. Growing evidence supports the connection between the dysregulation of STRIPAK complexes and cancer and other human diseases.

PP2A is a heterotrimeric Ser/Thr phosphatase that regulates numerous cellular processes. It has been shown that PP2A is dysregulated in several human diseases, including cancer. An essential role of PP2A as a tumor suppressor by controlling cell growth, and cancer development has also been studied.

In the current study, we have made several major findings based on the OS of the patients. First, we observed that high expressions of molecules resulted in an excellent indicator of poor STRN3, STRN4 and CALM were

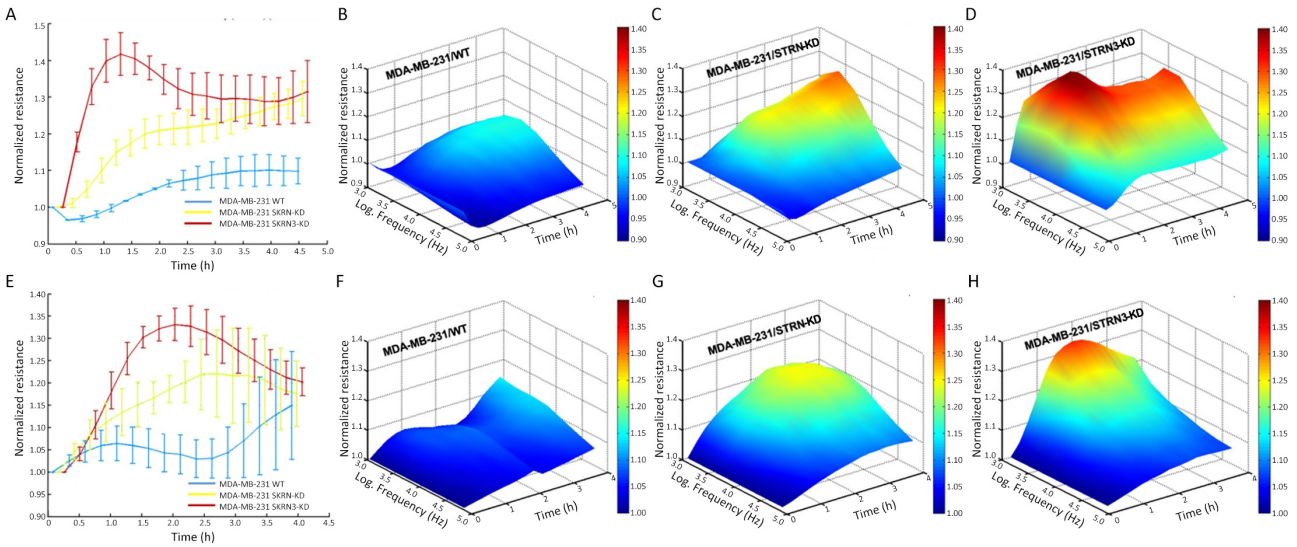

Figure 3 Cell adhesiveness and migration of MDA-MB-231 cells with different STRNs expressions, namely MDA-MB-231 WT, MDA-MB-231 STRN-KD and MDA-MB-231 STRN3-KD. (A–D) adhesion assay; (E–H) migration assay. From left to right, (A,E) 2D graph compares cell responses among cell models detected at 4,000 Hz (resistance with standard errors); (B,F) 3D graph of cell responses for WT cells; (C,G) 3D graph of cell responses for STRN-KD cells; (D,H) 3D graph of cell responses for STRN3-KD cells. The 3D figures indicate cell responses (Z-axis, normalized resistance in ohms) over time (X-axis, hours) and across multiple frequencies (Y-axis, Hz). All resistance detected was normalized with the initial result acquired. WT, wild type; KD, knockdown.

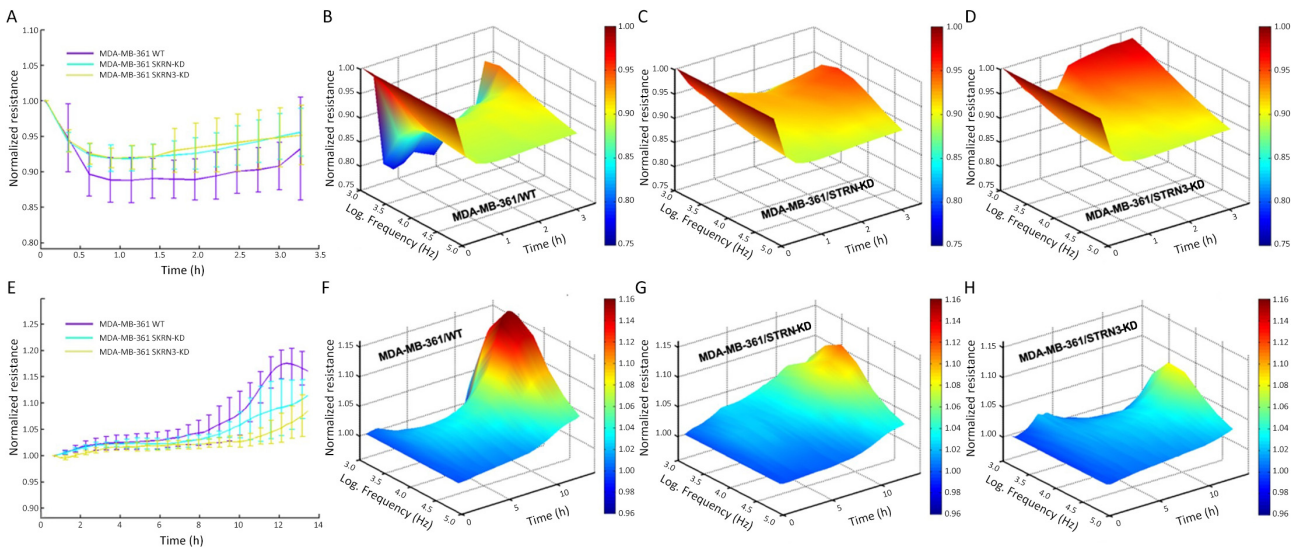

Figure 4 Cell adhesiveness and migration of MDA-MB-361 cells with different STRNs expressions, namely MDA-MB-361 WT, MDA-MB-361 STRN-KD and MDA-MB-361 STRN3-KD. (A–D) adhesion assay; (E–H) migration assay. From left to right, (A,E) 2D graph compares cell responses among cell models detected at 4,000 Hz (resistance with standard errors); (B,F) 3D graph of cell responses for WT cells; (C,G) 3D graph of cell responses for STRN-KD cells; (D,H) 3D graph of cell responses for STRN3-KD cells. The 3D figures indicate cell responses (Z-axis, normalized resistance in ohms) over time (X-axis, hours) and across multiple frequencies (Y-axis, Hz). All resistance detected was normalized with the initial result acquired. WT, wild type; KD, knockdown.

associated with shorter prognosis. Our finding is consistent with previous publications on overexpression of STRN3, STRN4 and is associated with poor prognosis of GC

CALM in some cancers. For example, in gastric cancer patients; *in vivo* experiments also confirmed that in CALM2 (GC) tissues and cell lines, CALM2 expression

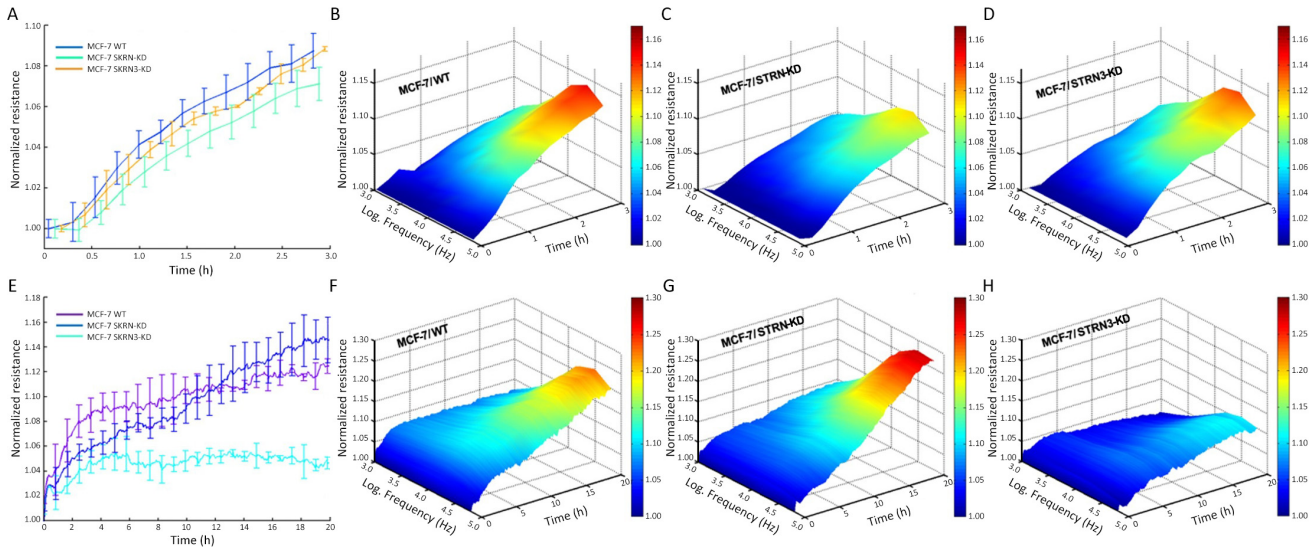

Figure 5 Cell adhesiveness and migration of MCF-7 cells with different STRNs expressions, namely MCF-7 WT, MCF-7 STRN-KD and MCF-7 STRN3-KD. (A–D) adhesion assay; (E–H) migration assay. From left to right, (A,E) 2D graph compares cell responses among cell models detected at 4,000 Hz (resistance with standard errors); (B,F) 3D graph of cell responses for WT cells; (C,G) 3D graph of cell responses for STRN-KD cells; (D,H) 3D graph of cell responses for STRN3-KD cells. The 3D figures indicate cell responses (Z-axis, normalized resistance in ohms) over time (X-axis, hours) and across multiple frequencies (Y-axis, Hz). All resistance detected was normalized with the initial result acquired. WT, wild type; KD, knockdown.

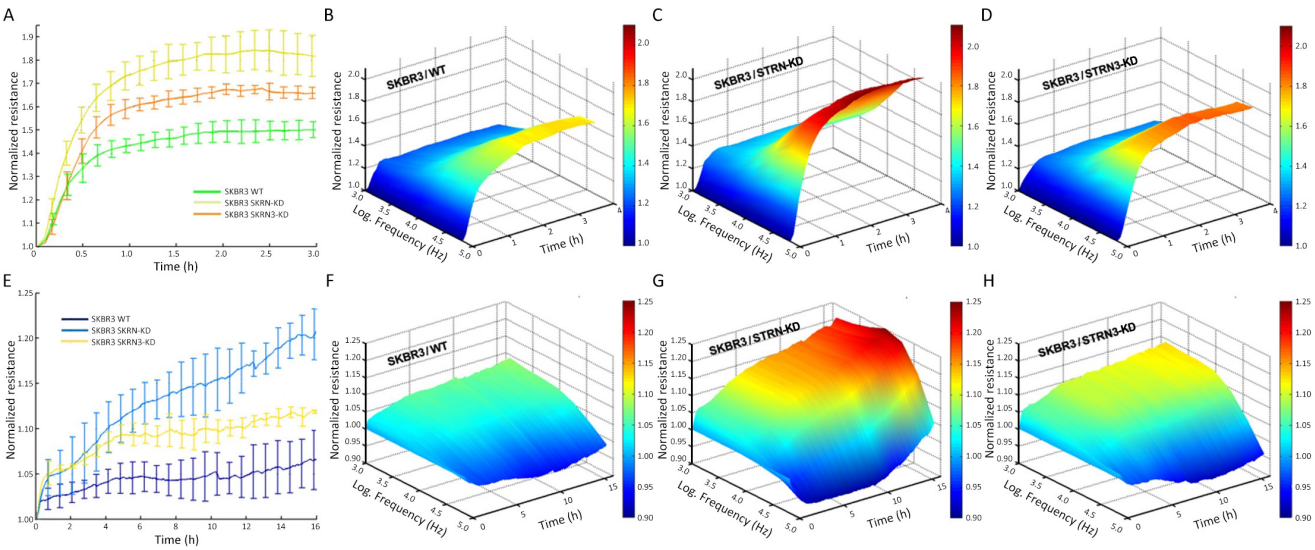

Figure 6 Cell adhesiveness and migration of SKBR3 cells with different STRNs expressions, namely SKBR3 WT, SKBR3 STRN-KD and SKBR3 STRN3-KD. (A–D) adhesion assay; (E–H) migration assay. From left to right, (A,E) 2D graph compares cell responses among cell models detected at 4,000 Hz (resistance with standard errors); (B,F) 3D graph of cell responses for WT cells; (C,G) 3D graph of cell responses for STRN-KD cells; (D,H) 3D graph of cell responses for STRN3-KD cells. The 3D figures indicate cells responses (Z-axis, normalized resistance in ohms) over time (X-axis, hours) and across multiple frequencies (Y-axis, Hz). All resistance detected was normalized with the initial result acquired. WT, wild type; KD, knockdown.

was boosted tumor growth and lung metastasis (35).

Secondly, we observed that higher levels of PPP2A, PPP2B and PPPR1A in patients with significantly longer OS; the combination of these three biomarkers leads to a favorable prognostic indicator. This finding is also consistent with the previous reports on PPP2A behaving as

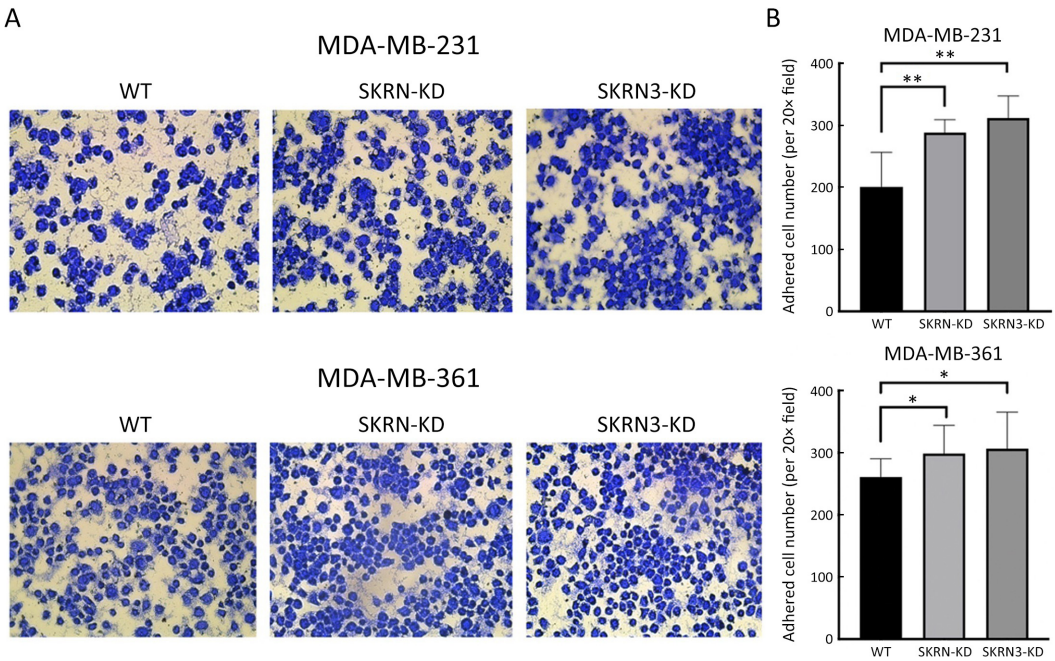

Figure 7 Matrigel adhesion assay of MDA-MB-231 (up) and MDA-MB-361 (bottom). (A) Representative images of adhered cells captured at 20× magnification; (B) Bar graphs of adhered cell number for each cell model (n=12). *, P<0.05; **, P<0.01 for comparisons between KD and WT cells. KD, knockdown, WT, wild type.

Table 8 IC_{50} of chemo-drugs tests

Variables	Paclitaxel (nmol/L)	Docetaxel (nmol/L)
MDA-MB-231/WT	58.6	24.3
MDA-MB-231/STRN-KD	167.0	31.9
MDA-MB-231/STRN3-KD	279.0	32.2
MDA-MB-361/WT	14.0	5.2
MDA-MB-361/STRN-KD	19.0	0.8
MDA-MB-361/STRN3-KD	14.2	5.3
MCF-7/WT	4.7	1.0
MCF-7/STRN-KD	0.7	0.6
MCF-7/STRN3-KD	2.6	6.5
SKBR3/WT	7.3	4.9
SKBR3/STRN-KD	0.1	13.6
SKBR3/STRN3-KD	9.0	0.4

a tumor suppressor. We have also found that integration of both STRNs group and PPP2 protein family members constitutes a highly significant prognostic indicator for both OS and DFS, which is independent of other factors (clinical, pathological, or receptor status). It was also interesting that the new biomarker signature, when combined with traditional markers including ER and Her2 can further identify the subgroups of patients with the worst survival, namely those with ER(−), Her2(+) and ER(−)/Her2(+) subtypes, affording additional value to this finding. This would need further validation in a much larger cohort of patients in the future.

Our *in vitro* study on cells' behaviour suggested that the expression of STRN and STRN3 could influence the cell-cell interaction during both cell adhesion and migration periods. According to a recent study which proposed that STRN contributes to both adherent junction and tight junctions (6), further *in vitro* studies could be conducted to assess the integrity and barrier functions of epithelial cells in various epithelial tissues after STRNs knockdown.

By analyzing the clinical results, we also observed that higher STRN3 expression was strongly associated with better tumor pathological responses to chemotherapy in patients who exhibited ER(+)/Her2(−) status, in contrast to the ER(−)/Her2(+) group in which high expression of STRN3 was associated with greater resistance to chemo-drugs. This observation was aligned with our *in-vitro* chemo-drug test of MCF-7 [ER(+)/Her2(−)] and SKBR3 [ER(−)/Her2(+)] cells' responses to one of the chemo-drug tested, namely Docetaxel. Interestingly, there was no difference in IC_{50} values between WT MDA-MB-361 [ER(+)/Her2(+)] and the STRN3-KD cells when they were treated with docetaxel or paclitaxel. Whilst our clinical results indicated that patients with ER(+)/Her2(+) showed

better response to chemotherapies when they had lower STRN3 expression, we also found that higher expression of STRN3 was associated with increased drug sensitivity in patients with Her2(+) cancers (*Table 8*). The combined impact of the receptor status in response to chemotherapies might thereby explain our results. Thus, the present study has provided some important information on the link between the STRIPAK and STRNs in evaluating patients' clinical response to drug therapies.

However, the present study has its limitations. The expression analysis was conducted on a historical collection of fresh frozen tissues. The present study has an advantage in that the tested molecules were free from the influence of drug intervention as none of the patients received neoadjuvant therapy prior to surgery. It would be, however, ideal to validate the study on an independent cohort, similarly unaffected by the pre-surgery treatment. This option was not available to the present study, and we hope in future that carefully selected datasets from a public database would be available to help address this limitation. Additionally, it is essential to investigate the mechanistic role of STRIPAK in chemo-resistance at the protein level by looking into the signaling events that the STRIPAK complex involved, such as the Hippo signal pathway. It has been shown that the Hippo-STRIPAK complex plays an essential role in regulating DNA double-stranded break repair and genomic stability (16). Thus, a future project would be needed to examine the possible contribution of the STRIPAK signature and mutations of the gene related to these pathways including the homologous recombination repair (*HRR*) genes and the homologous recomination deficiency genes (*HRD*) to patients' response to drugs such as the PARP inhibitors. STE20-like protein kinases 1 and 2 (MST1/2) have also been reported to directly phosphorylate the zinc finger MYND type-containing 8 or ZMYND8, leading to the suppression of DNA repair in the nucleus. However, MST1/2 inactivation by STRIPAK could increase the DNA repair capacity and contribute to chemo-resistance in cancer cells. In contrast, STRIPAK inhibitors could recover the kinase activity of MST1/2, resulting in re-sensitization of cancer cells to chemotherapy.

Conclusions

The integrated profile of STRNs and the key STRIPAK members presents a significant opportunity in evaluating the prognosis in patients with breast cancer. STRNs especially STRN3 is also a highly valuable indicator to patient's response to chemotherapies, which is highly depended on the hormonal receptor status and molecular subtypes. Since STRN3 functions as a cornerstone of the STRIPAK complex, finding an inhibitor to STRN3 that could disrupt the formation and stability of the complex would be plausible for the therapeutic consideration in the treatment of STRIPAK-related cancers.

Acknowledgements

The study was supported by the Cardiff University China Medical Scholarship.

Footnote

Conflicts of Interest: The authors have no conflicts of interest to declare.

References

1. Muro Y, Chan EK, Landberg G, et al. A cell-cycle nuclear autoantigen containing WD-40 motifs expressed mainly in S and G2 phase cells. Biochem Biophys Res Commun 1995;207:1029-37.
2. Castets F, Bartoli M, Barnier JV, et al. A novel calmodulin-binding protein, belonging to the WD-repeat family, is localized in dendrites of a subset of CNS neurons. J Cell Biol 1996;134:1051-62.
3. Castets F, Rakitina T, Gaillard S, et al. Zinedin, SG2NA, and striatin are calmodulin-binding, WD repeat proteins principally expressed in the brain. J Biol Chem 2000;275:19970-7.
4. Gaillard S, Bartoli M, Castets F, et al. Striatin, a calmodulin-dependent scaffolding protein, directly binds caveolin-1. FEBS Lett 2001;508:49-52.
5. Nader M, Alotaibi S, Alsolme E, et al. Cardiac striatin interacts with caveolin-3 and calmodulin in a calcium sensitive manner and regulates cardiomyocyte spontaneous contraction rate. Can J Physiol Pharmacol 2017;95:1306-12.
6. Lahav-Ariel L, Caspi M, Nadar-Ponniah PT, et al. Striatin is a novel modulator of cell adhesion. FASEB J 2019;33:4729-40.
7. Goudreault M, D'Ambrosio LM, Kean MJ, et al. A PP2A phosphatase high density interaction network identifies a novel striatin-interacting phosphatase and kinase complex linked to the cerebral cavernous

malformation 3 (CCM3) protein. Mol Cell Proteomics 2009;8:157-71.
8. Hwang J, Pallas DC. STRIPAK complexes: structure, biological function, and involvement in human diseases. Int J Biochem Cell Biol 2014;47:118-48.
9. Kean MJ, Ceccarelli DF, Goudreault M, et al. Structure-function analysis of core STRIPAK proteins: a signaling complex implicated in Golgi polarization. J Biol Chem 2011;286:25065-75.
10. Kück U, Radchenko D, Teichert I. STRIPAK, a highly conserved signaling complex, controls multiple eukaryotic cellular and developmental processes and is linked with human diseases. Biol Chem 2019;400: 1005-22.
11. Hyodo T, Ito S, Hasegawa H, et al. Misshapen-like kinase 1 (MINK1) is a novel component of striatin-interacting phosphatase and kinase (STRIPAK) and is required for the completion of cytokinesis. J Biol Chem 2012;287:25019-29.
12. Gordon J, Hwang J, Carrier KJ, et al. Protein phosphatase 2a (PP2A) binds within the oligomerization domain of striatin and regulates the phosphorylation and activation of the mammalian Ste20-Like kinase Mst3. BMC Biochem 2011;12:54.
13. Nordzieke S, Zobel T, Fränzel B, et al. A fungal sarcolemmal membrane associated protein (SLMAP) homolog plays a fundamental role in development and localizes to the nuclear envelope, endoplasmic reticulum, and mitochondria. Eukaryot Cell 2015;14: 345-58.
14. Schad EG, Petersen CP. STRIPAK limits stem cell differentiation of a WNT signaling center to control planarian axis scaling. Curr Biol 2020;30:254-63.e2.
15. Lu J, Hu Z, Deng Y, et al. MEKK2 and MEKK3 orchestrate multiple signals to regulate Hippo pathway. J Biol Chem 2021;296:100400.
16. An L, Cao Z, Nie P, et al. Combinatorial targeting of Hippo-STRIPAK and PARP elicits synthetic lethality in gastrointestinal cancers. J Clin Invest 2022;132: e155468.
17. Breitman M, Zilberberg A, Caspi M, et al. The armadillo repeat domain of the APC tumor suppressor protein interacts with Striatin family members. Biochim Biophys Acta 2008;1783:1792-802.
18. Zheng S, Sun P, Liu H, et al. 17β-estradiol upregulates striatin protein levels via Akt pathway in human umbilical vein endothelial cells. PLoS One 2018;13:e0202500.
19. Belachew EB, Sewasew DT. Molecular mechanisms of endocrine resistance in estrogen-positive breast cancer. Front Endocrinol (Lausanne) 2021;12:599586.
20. Xie R, Wen F, Qin Y. The dysregulation and prognostic analysis of STRIPAK complex across cancers. Front Cell Dev Biol 2020;8:625.
21. Czauderna C, Poplawski A, O'Rourke CJ, et al. Epigenetic modifications precede molecular alterations and drive human hepatocarcinogenesis. JCI Insight 2021;6:e146196.
22. Ito M, Hiwasa T, Oshima Y, et al. Identification of serum anti-striatin 4 antibodies as a common marker for esophageal cancer and other solid cancers. Mol Clin Oncol 2021;15:237.
23. Kelly LM, Barila G, Liu P, et al. Identification of the transforming STRN-ALK fusion as a potential therapeutic target in the aggressive forms of thyroid cancer. Proc Natl Acad Sci U S A 2014;111:4233-8.
24. Qiu LM, Sun YH, Chen TT, et al. STRIP2, a member of the striatin-interacting phosphatase and kinase complex, is implicated in lung adenocarcinoma cell growth and migration. FEBS Open Bio 2020;10: 351-61.
25. Wong M, Hyodo T, Asano E, et al. Silencing of STRN4 suppresses the malignant characteristics of cancer cells. Cancer Sci 2014;105:1526-32.
26. Gupta R, Kumar G, Jain BP, et al. Ectopic expression of 35 kDa and knocking down of 78 kDa SG2NAs induce cytoskeletal reorganization, alter membrane sialylation, and modulate the markers of EMT. Mol Cell Biochem 2021;476:633-48.
27. Bisoyi P, Devi P, Besra K, et al. The profile of expression of the scaffold protein SG2NA(s) differs between cancer types and its interactome in normal vis-a-vis breast tumor tissues suggests its wide roles in regulating multiple cellular pathways. Mol Cell Biochem 2022;477:1653-68.
28. Lu Q, Pallas DC, Surks HK, et al. Striatin assembles a membrane signaling complex necessary for rapid, nongenomic activation of endothelial NO synthase by estrogen receptor alpha. Proc Natl Acad Sci U S A 2004;101:17126-31.
29. Tan B, Long X, Nakshatri H, et al. Striatin-3 gamma inhibits estrogen receptor activity by recruiting a

protein phosphatase. J Mol Endocrinol 2008;40: 199-210.
30. Jiang WG, Watkins G, Lane J, et al. Prognostic value of rho GTPases and rho guanine nucleotide dissociation inhibitors in human breast cancers. Clin Cancer Res 2003;9:6432-40.
31. Giaever I, Keese CR. Micromotion of mammalian cells measured electrically. Proc Natl Acad Sci U S A 1991;88:7896-900.
32. Yang Y, Sanders AJ, Ruge F, et al. Activated leukocyte cell adhesion molecule (ALCAM)/CD166 in pancreatic cancer, a pivotal link to clinical outcome and vascular embolism. Am J Cancer Res 2021;11: 5917-32.
33. Frugtniet BA, Martin TA, Zhang L, et al. Neural Wiskott-Aldrich syndrome protein (nWASP) is implicated in human lung cancer invasion. BMC Cancer 2017;17:224.
34. Fekete JT, Győrffy B. ROCplot. org: Validating predictive biomarkers of chemotherapy/hormonal therapy/anti-HER2 therapy using transcriptomic data of 3,104 breast cancer patients. Int J Cancer 2019;145: 3140-51.
35. Mu G, Zhu Y, Dong Z, et al. Calmodulin 2 facilitates angiogenesis and metastasis of gastric cancer via STAT3/HIF-1A/VEGF-A mediated macrophage polarization. Front Oncol 2021;11:727306.

Cite this article as: Li AX, Zeng JJ, Martin TA, Ye L, Ruge F, Sanders AJ, Khan E, Dou P, Davies E, Jiang W. Striatins and STRIPAK complex partners in clinical outcomes of patients with breast cancer and responses to drug treatment. Chin J Cancer Research 2023;35(4):365-385. doi: 10.21147/j.issn.1000-9604.2023.04.04

Table S1 PCR primers

Molecule	Forward (5'–3')	Reverse (5'–3')*
STRIP1	tgctttgaggaggacttc	**actgaacctgaccgtaca**gacttccaagccatccag
STRIP2	gtatggagatgcagatggg	**actgaacctgaccgtaca**cttcaaagcacctcctgt
MOB4	tatggtcatggcggagg	**actgaacctgaccgtacac**aaaggattcatcaggcca
CCM3 (PDCD10)	ccatggtttctatgcccc	**actgaacctgaccgtaca**cttgatgaaagcggctct
SIKE1	gagtcgctggtggatca	**actgaacctgaccgtaca**gtccttcatatcggatgca
MINK1	cctactacggagccttca	**actgaacctgaccgtaca**taggcgatacagtcctcc
SLMAP	tggagtagacgtgacaga	**actgaacctgaccgtaca**gggcttccataccatctg
STRN3	actgggaggtggaacg,	**actgaacctgaccgtaca**tccttcttcaggttctcttg
STRN	ggaaacaaggtcgacaact	**actgaacctgaccgtaca**cgcactcgtttagatttca
STRN4	ggtcaccctggagaaca	**actgaacctgaccgtaca**gtctgtgtagcccacctct
PPP2CA	ggagattatgttgacagagga	**actgaacctgaccgtaca**ctcgaagaatggtgatgc
PPP2CB	gagactgtgactcttcttgt	**actgaacctgaccgtaca**cggctttcgtgatttcct
PPP2R1A	ggcaaagacaacaccatc	**actgaacctgaccgtaca**cgttcacacagtccaggt
PPP2R4	tccacacagttccagaca	**actgaacctgaccgtaca**actcgaaggtcagcttct
MST1 (HGFL)	gaccagccgccatcaatc	**actgaacctgaccgtaca**cttggaacgccgctgatc
MST1R (RON)	catccacccagtgccaac	**actgaacctgaccgtaca**ccacacagtcagccacag
TNKS1	ccttttccctcactcgat	**actgaacctgaccgtaca**ccaccgagtcactgtctt
TNKS2	ctggtgacgcctgagaag	**actgaacctgaccgtaca**gtctttccgcccaaaacc
Caveolin	**actgaacctgaccgtaca**aacacgtagctgcccttc	cttgtagatgttgccctgtt
GAPDH	aaggtcatccatgacaactt	**actgaacctgaccgtaca**gccatccacagtcttctg
CK19	agccactactacacgaccat	**actgaacctgaccgtaca**tcgatctgcaggacaatc

*, Z-sequence for qPCR analysis; qPCR, real-time quantitative polymerase chain reaction.